Nuclear Medicine and Biology 40 (2013) 481–487

Contents lists available at SciVerse ScienceDirect

Nuclear Medicine and Biology

journal homepage: www.elsevier.com/locate/nucmedbio

Design and biological evaluation of ^{99m}Tc-N_2S_2-Tat(49–57)-c(RGDyK): A hybrid radiopharmaceutical for tumors expressing α(v)β(3) integrins

Blanca E. Ocampo-García [a], Clara L. Santos-Cuevas [a], Luis M. De León-Rodríguez [b], Rocío García-Becerra [c], David Ordaz-Rosado [c], Myrna A. Luna-Guitiérrez [a,d], Nallely P. Jiménez-Mancilla [a,d], Mario E. Romero-Piña [e], Guillermina Ferro-Flores [a,*]

[a] Departamento de Materiales Radiactivos, Instituto Nacional de Investigaciones Nucleares, Estado de México, Mexico
[b] Departamento de Química, Universidad de Guanajuato, Guanajuato, Mexico
[c] Instituto Nacional de Ciencias Médicas y Nutrición Salvador Zubirán, México D.F., Mexico
[d] Facultad de Medicina, Universidad Autónoma del Estado de México, Estado de México, Mexico
[e] Departamento de Investigación Básica, Instituto Nacional de Cancerología, México D.F., Mexico

ARTICLE INFO

Article history:
Received 30 December 2012
Received in revised form 8 January 2013
Accepted 15 January 2013

Keywords:
Radiolabeled RGD
Hybrid radiopharmaceutical
^{99m}Tc-Tat-RGD
Tat-RGD

ABSTRACT

The α(ν)β(3) integrin is over-expressed in the tumor neovasculature and the tumor cells of glioblastomas. The HIV Tat-derived peptide has been used to deliver various cargos into cells. The aim of this research was to synthesize and assess the *in vitro* and *in vivo* uptake of ^{99m}Tc-N_2S_2-Tat(49–57)-c(RGDyK) (^{99m}Tc-Tat-RGD) in α(ν)β(3) integrin positive cancer cells and compare it to that of a conventional ^{99m}Tc-RGD peptide (^{99m}Tc-EDDA/HYNIC-E-[c(RGDfK)]$_2$). *Methods:* The c(RGDyK) peptide was conjugated to a maleimidopropionyl (MP) moiety through Lys, and the MP group was used as the branch position to form a thioether with the Cys^{12} side chain of the Tat(49–57)-spacer-N_2S_2 peptide. ^{99m}Tc-Tat-RGD was prepared, and stability studies were carried out by size exclusion HPLC analyses in human serum. The *in vitro* affinity for α(ν)β(3) integrin was determined by a competitive binding assay. *In vitro* internalization was determined using glioblastoma C6 cells. Biodistribution studies were accomplished in athymic mice with C6 induced tumors that had blocked and unblocked receptors. Images were obtained using a micro-SPECT/CT. *Results*: ^{99m}Tc-Tat-RGD was obtained with a radiochemical purity higher than 95%, as determined by radio-HPLC and ITLC-SG analyses. Protein binding was 15.7% for ^{99m}Tc-Tat-RGD and 5.6% for ^{99m}Tc-RGD. The IC_{50} values were 6.7 nM (^{99m}Tc-Tat-RGD) and 4.6 nM (^{99m}Tc-RGD). Internalization in C6 cells was higher in ^{99m}Tc-Tat-RGD (37.5%) than in ^{99m}Tc-RGD (10%). Biodistribution studies and *in vivo* micro-SPECT/CT images in mice showed higher tumor uptake for ^{99m}Tc-Tat-RGD (6.98% ± 1.34% ID/g at 3 h) than that of ^{99m}Tc-RGD (3.72% ± 0.52% ID/g at 3 h) with specific recognition for α(ν)β(3) integrins. *Conclusions*: Because of the significant cell internalization (Auger and internal conversion electrons) and specific recognition for α(ν)β(3) integrins, the hybrid ^{99m}Tc-N_2S_2-Tat(49–57)-c(RGDyK) radiopharmaceutical is potentially useful for the imaging and possible therapy of tumors expressing α(ν)β(3) integrins.

1. Introduction

Cell penetrating peptides (CPPs) are short peptides that can efficiently cross the plasma membrane of a living cell and are under development as delivery vehicles for therapeutic agents that cannot enter the cell themselves [1]. One well-studied CPP is Tat(49–57) derived from the human immunodeficiency virus type 1 (HIV-1) Tat protein. It has been well studied as an effective CPP and an attractive drug delivery agent [1–3]. The Tat(49–57) peptide is comprised of six arginine and two lysine residues, as well as one non-ionic amino acid (total charge +8). Different studies have determined that the activity of Tat(49–57) as a CPP involves interactions with the cellular membrane and cytoskeleton, and it is influenced by numerous variables related to the peptide, the cargo, and extracellular conditions [4].

At the single-cell level, short-range charged particles, such as internal conversion (IC) and Auger electrons, impart a dense ionizing energy deposition pattern associated with increased radiobiological effectiveness. However, they must be able to penetrate into the cytoplasm and

* Corresponding author. Departamento de Materiales Radiactivos, Instituto Nacional de Investigaciones Nucleares, Carretera México-Toluca S/N, La Marquesa, Ocoyoacac, Estado de México, C.P. 52750, México. Tel.: +52 55 53297200x3863; fax: +52 55 53297306.
E-mail addresses: ferro_flores@yahoo.com.mx, guillermina.ferro@inin.gob.mx (G. Ferro-Flores).

0969-8051/$ – see front matter © 2013 Elsevier Inc. All rights reserved.
http://dx.doi.org/10.1016/j.nucmedbio.2013.01.003

reach the nucleus, which is considered to be the most radiosensitive component of the cell. Auger and IC electron emitters that can be targeted to the DNA of tumor cells represent an attractive system of radiation therapy because of their high linear energy transfer (LET) within nuclear dimensions (4 to 26 keV/μm) [5]. Auger and IC radiations have low toxicity when they decay outside the cell nucleus, for example, in the cytoplasm or outside cells during blood transport. Technetium-99 m (^{99m}Tc) produces Auger energy of 0.90 keV/decay and IC electron energy of 15.40 keV/decay, which represent 11.4% of the total ^{99m}Tc energy released per decay [5,6].

Angiogenesis is a physiological process involving tumor growth and metastasis. The angiogenic process is regulated by cell adhesion receptors, such as integrins. The $\alpha(\nu)\beta(3)$ integrin is expressed on the surface of normal endothelial cells at low levels, but it is overexpressed in the tumor neovasculature and tumor cells of osteosarcoma, neuroblastoma, glioblastoma, melanoma, lung carcinoma and breast cancer [7,8]. Radiolabeled peptides based on the Arg-Gly-Asp (RGD) sequence have been reported as radiopharmaceuticals with high affinity and selectivity for the $\alpha(\nu)\beta(3)$ integrin and are therefore useful in the non-invasive monitoring of tumor angiogenesis by molecular imaging techniques [9–12]. A hybrid radiopharmaceutical of type ^{99m}Tc-N_2S_2-Tat(49–57)-c(RGDyK) would significantly increase cancer cell uptake and, consequently, image contrast of cancer tumors and their metastases, which would improve sensitivity and specificity of diagnostic studies. Furthermore, internalizing IC and Auger electrons in the nucleus of a malignant cell could increase the effectiveness of targeted radiotherapy [13].

The aim of this research was to prepare and assess the *in vitro* and *in vivo* uptake of ^{99m}Tc-N_2S_2-Tat(49–57)-c(RGDyK) in $\alpha(\nu)\beta(3)$ integrin positive cancer cells and compare the cellular uptake to that of a conventional ^{99m}Tc-RGD peptide (^{99m}Tc-EDDA/HYNIC-E-[c(RGDfK)]$_2$).

2. Materials and methods

2.1. General

The c(RGDyK) peptide was conjugated to a maleimidopropionyl (MP) moiety through the Lys, and the MP group was used as the branch position to form a thioether with the Cys^{12} side chain of the Tat(49–57)-spacer-N_2S_2 peptide (Fig. 1).

Mass spectra (MS) were collected on an Applied Biosystems Voyager-6115 [matrix-assisted laser desorption/ionization time-of-flight (MALDI-TOF)] mass spectrometer in positive linear mode using alpha-cyano-4-hydroxycinnamic acid as the matrix. High performance liquid chromatography (HPLC) purification was performed on an Agilent 1200 system using a semi-preparative Luna (10 μm, C18, 300 Å, 250 mm × 10 mm column from Phenomenex. Analytical HPLC was performed using a Luna 5 μm, C18, 300 Å, 250 mm × 4.6 mm column. Compound elution was monitored by UV–vis at 235 nm unless otherwise stated.

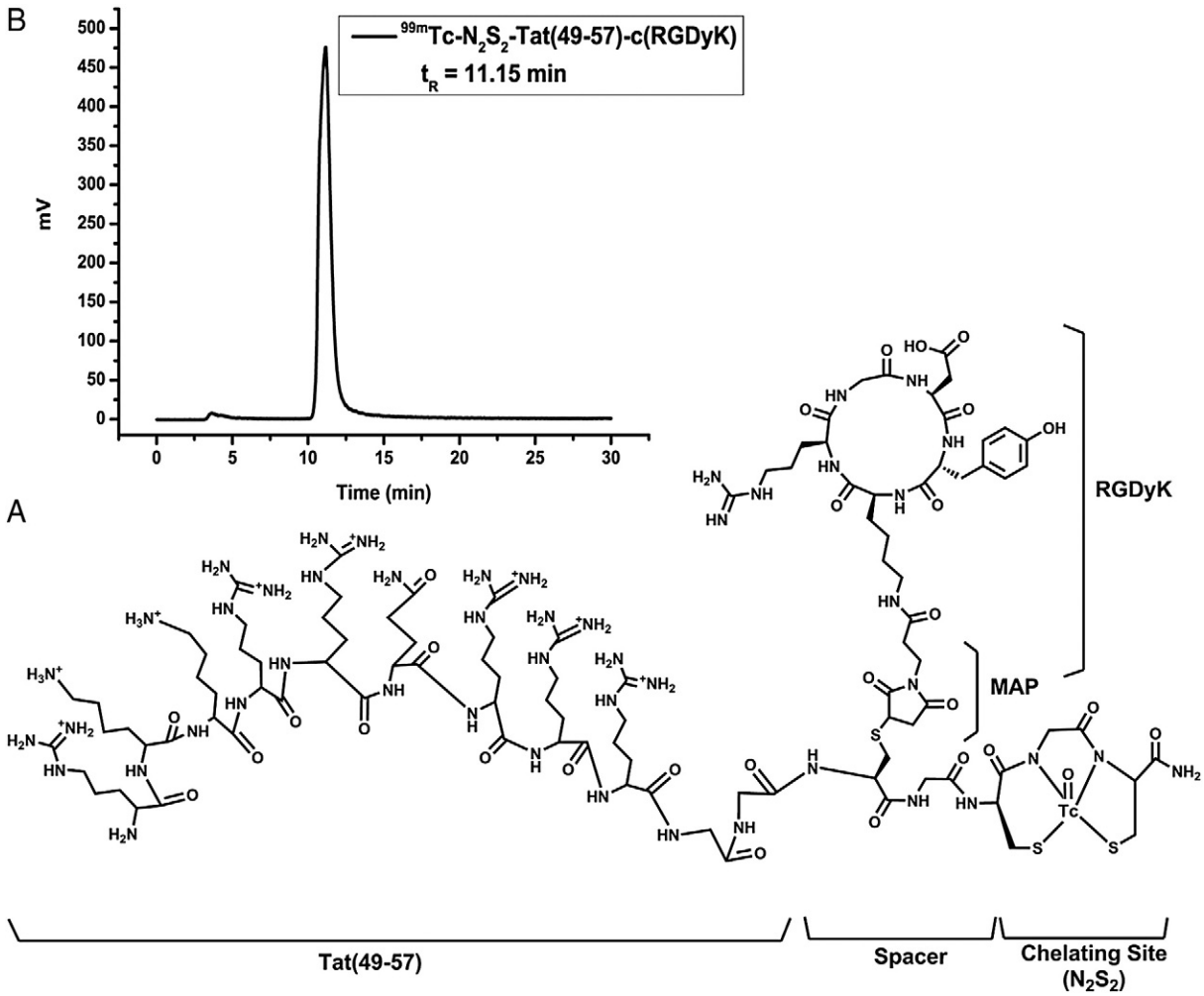

Fig. 1. General scheme of the N_2S_2-Tat(49–57)-c(RGDyK) hybrid peptide labeled with ^{99m}Tc. Reverse phase radio-HPLC chromatogram of the ^{99m}Tc-N_2S_2-Tat(49–57)-c(RGDyK) radiopharmaceutical (top-left).

2.2. Chemistry

2.2.1. Synthesis of c(Arg-Gly-Asp-$_D$Tyr-Lys)-3-maleimidepropionylamide (c(RGDyK)-3MP)

The synthesis of the linear peptide started with the conjugation of glycine to *o*-chlorotrityl chloride resin (Advanced ChemTech, 0.9 mmol/g load) at a 1.29 mmol scale by mixing the resin with a solution of Fmoc-Gly-OH (975 mg, 2.5 equiv) and N,N-diisopropylethylamine (DIPEA) (492 μL, 1.15 equiv) in dry dichloromethane (DCM) in a peptide synthesis vessel. After shaking the reaction mixture for 2.5 h, the mixture was removed, and the resin was washed with dimethylformamide (DMF) and DCM. The load of the resin was determined by HPLC via quantification of the Fmoc group after removal by piperidine from 4.1 mg of dry resin. The load of the resin was 0.69 mmol (54%). DIPEA (730 μL) in 4 mL of methanol was added to the resin to cap the unreacted sites on the resin. After 1 h, the resin was washed with DMF and DCM. The Fmoc-protecting group was then removed with a 20% solution of piperidine in DMF. Amino acids were then attached using single-step couplings of 3.5 equiv. of the Fmoc-amino acid, 3.4 equiv of *o*-(benzotriazol-1-yl)-N,N,N′,N′-tetramethyluronium hexafluorophosphate (HBTU) and N-hydroxybenzotriazole (HOBt), and 5.0 equiv of DIPEA in DMF in the following order: Fmoc-Arg(Pbf)-OH, Fmoc-Lys(Boc)-OH, Fmoc-D-Tyr-OH, and Fmoc-Asp(OtBu)-OH, for 2 h each. The linear RGDyK peptide was cleaved from the resin without affecting other protecting groups by treating with 10 mL of a mixture of acetic acid, 2,2,2-trifluoroethanol, and DCM (1:1:3) for 1.7 h at room temperature. The solution was filtered, the resin washed twice with 5 mL of the same mixture and then washed with DCM three times. The filtrates were combined and concentrated. The excess acetic acid was removed by repeatedly adding hexanes to the residue and removing the mixture by rotary evaporation. The head-to-tail cyclization was performed by slowly adding a solution containing 612 mg of the linear peptide in 6.4 mL of DCM to a solution of 50% 1-propanephosphonic acid cyclic anhydride in ethyl acetate (2.7 mL), DIPEA (2.3 mL), and 4-(N,N-dimethylamino)pyridine (5.0 mg) in 250 mL of DCM. After stirring overnight, the reaction mixture was concentrated and purified by silica chromatography (1:10 methanol:ethyl acetate, followed by 1:5 methanol:ethyl acetate). Fractions containing the product were collected, and the solvent was removed by rotary evaporation. DCM was added to the residue and then washed with water. The organic phase was collected and the solvent removed. The remaining protecting groups of the above cyclic peptide were removed by stirring the peptide for 2 h with a mixture of 95% trifluoroacetic acid (TFA) and 5% water. The excess TFA was removed under a gentle flow of N_2. Cold diethyl ether was added to the residue giving a white precipitate. Ether was decanted, and the solid washed 3× with fresh cold ether. The dried solid was white with a 480 mg yield. HPLC of the peptide with a gradient of water/acetonitrile containing 0.1 and 0.08% TFA, respectively, from 90/10 to 30/70 in 25 min at a flow rate of 1 mL/min gave two peaks with $t_R = 5.2$ and 6.7 min. The major peak corresponded to the fully deprotected c(RGDyK) peptide [m/z (MALDI+) = 620.41 $[M+H]^+$ (calc. 620.67)], and the minor peak corresponded to the Pbf protected peptide [m/z (MALDI+) = 872.53 $[M+H]^+$ (calc. 873.00)].

Then, 51.5 mg (0.95 equiv.) of 3-maleimidepropionic acid, 50.3 μL of DIPEA (1 equiv.) and 115.5 mg HBTU were dissolved in 0.8 mL DMF. The mixture was stirred at room temperature for 5 min resulting in formation of a white precipitate. This solution was added to another solution consisting of 270 mg (0.32 mmol) of the ditrifluoroacetate salt of the c(RGDyK) peptide and 105 μL DIPEA (2 equiv.) in 1 mL DMF. The solution was stirred at room temperature and the precipitate observed above disappeared, yielding a yellowish transparent solution. The reaction was completed after 5 min as assessed by HPLC. The product was purified via semi-preparative HPLC with a gradient of water/acetonitrile containing 0.1% and 0.08% TFA, respectively, from 90/10 to 30/70 in 30 min at a flow rate of 4.7 mL/min. The peptide eluted at $t_R = 14.1$ min from an analytical HPLC column using a gradient of water/acetonitrile containing 0.1% and 0.08% TFA, respectively, from 95/5 to 10/90 in 30 min at a flow rate of 1 mL/min at room temperature [m/z (MALDI+) = 771.54 $[M+H]^+$ (calc. 771.79)].

2.2.2. Synthesis of NH_2-Arg-Lys-Lys-Arg-Arg-Gln-Arg-Arg-Arg-Gly-Gly-Cys-Gly-Cys(Acm)-Gly-Cys(Acm)-$CONH_2$ (N_2S_2-Tat(49–57))

The synthesis of the peptide started with the incorporation of Fmoc-Cys(Acm) onto a NovaSynTGR resin (Novabiochem, 0.2 mmol/g load) on a 0.3 mmol scale. Peptide synthesis continued following standard solid phase peptide synthesis protocols (SPPS). Protecting groups and removal of the peptide from the resin were accomplished by stirring the resin in a mixture of TFA/triisopropylsilane/H_2O (95/2.5/2.5) for 4 h. (It is important not to use thiol-containing scavengers because these remove the Acm protecting group.). N_2S_2-Tat(49–57) was eluted at $t_R = 12.8$ min from an analytical HPLC column using a gradient of water/acetonitrile containing 0.1% and 0.08% TFA, respectively, from 95/5 to 10/90 in 30 min at a flow rate of 1 mL/min at room temperature. The peptide was purified and provided 232 mg (75% yield, calculated based on the salt free peptide MW). [N_2S_2-Tat(49–57); m/z (MALDI+) = 2019.04 $[M+H]^+$ (calc. 2019.40)].

2.2.3. Synthesis of NH_2-Arg-Lys-Lys-Arg-Arg-Gln-Arg-Arg-Arg-Gly-Gly-Cys-[c(Arg-Gly-Asp-$_D$Tyr-Lys)-3-succinimidepropionylamide)]-Gly-Cys(Acm)-Gly-Cys(Acm)-$CONH_2$ (N_2S_2-Tat(49–57)-c(RGDyK))

N_2S_2-Tat(49–57) peptide (220 mg, 0.055 mmol) was mixed with 22.4 mg (0.4 equiv.) of c(RGDyK)-3MP in 3 mL of 0.1 M degassed phosphate buffer, pH 7.0, which contained 5 mM EDTA. The cyclic peptide was used as the limiting reagent because its use facilitates the purification of the final conjugate, which elutes very closely to the cyclic peptide. The reaction mixture was stirred at room temperature overnight. The solution was filtered through a PTFE 0.2 μm filter, and the product was purified by semi-preparative HPLC using an isocratic system from 0 to 6 min with water/acetonitrile containing 0.1% and 0.08% TFA, respectively. and 95/5, followed by a gradient to 80/20 from 6 to 30 min. Fractions containing the product were combined and freeze-dried, giving 66 mg of a white solid. The peptide eluted at $t_R = 13.6$ min from an analytical HPLC column, using a gradient of water/acetonitrile containing 0.1% and 0.08% TFA from 95/5 to 10/90 in 30 min at a flow rate of 1 mL/min at room temperature. [m/z (MALDI+) = 2791.34$[M+H]^+$ (calc. 2790.20)].

2.3. Radiochemistry

2.3.1. Radiolabeling of N_2S_2-Tat(49–57)-c(RGDyK)

Technetium-99 m: ^{99m}Tc-pertechnetate was obtained from a GETEC ^{99}Mo/^{99m}Tc generator (ININ, Ocoyoacac, Mexico).

One milligram of N_2S_2-Tat(49–57)-c(RGDyK) was dissolved in 200 μL of injectable water (Pisa®, Mexico). Ten microliters of this solution was added to 25 μL of sodium ^{99m}Tc-pertechnetate (185 MBq), followed by 7 μL of the acetamidomethyl (Acm) group deprotection mixture (50 mg/mL sodium tartrate in 0.1 M NH_4OH/NH_4CH_3COOH, pH 9.5) and 3 μL of reducing solution (0.5 mg $SnCl_2$/mL in 0.05 M HCl). The final mixture was incubated for 20 min at room temperature. After incubation, the solution was diluted to 2.5 mL with 0.9% NaCl.

2.3.2. Evaluation of ^{99m}Tc-N_2S_2-Tat(49–57)-c(RGDyK) radiochemical purity

Radiochemical purity analyses were performed by instant thin-layer chromatography on silica gel (ITLC-SG, Gelman Sciences) and reverse phase HPLC.

ITLC-SG analysis was accomplished using two different mobile phases: saline solution to determine the amount of free $^{99m}TcO_4^-$

($R_f = 1$) and 0.1 M sodium citrate, pH 5, to determine the amount of ^{99m}Tc-tartrate ($R_f = 1$). The R_f value of the radiolabeled peptide in each system was 0.0.

HPLC analyses were carried out with a Waters instrument running Millennium software with both radioactivity and UV-photodiode array in-line detectors and a μBondapak C_{18} column (5 μm, 3.9×300 mm). A gradient using 0.1% TFA/water as solvent A and 0.1% TFA/acetonitrile as solvent B was used at a flow rate of 1 mL/min. The gradient began at 100% solvent A for 3 min, changed to 50% solvent A over 10 min and was maintained for 10 min, changed to 30% solvent A over 3 min and finally returned to 100% solvent A over 4 min. Using this system, the retention times for free $^{99m}TcO_4^-$ and ^{99m}Tc-N_2S_2-Tat(49–57)-c(RGDyK) were 3 to 4 min and 10 to 11 min, respectively.

2.3.3. Preparation of ^{99m}Tc-EDDA/HYNIC-E-[c(RGDfK)]$_2$

As previously reported for HYNIC-peptides, a lyophilized formulation containing HYNIC-E-[c(RGDfK)]$_2$ (Pichem Co., Austria), EDDA, tricine, and stannous chloride was prepared (Ferro-Flores et. al., 2006). The radiolabeling procedure was carried out by adding 1 mL of 0.2 M phosphate buffer, pH 7.0, to the freeze-dried kit formulation and immediately adding 740–1110 MBq (1 mL) of ^{99m}Tc-pertechnetate, followed by incubation in boiling water for 15 min. Radiochemical purity was also evaluated by reverse phase HPLC as described above.

2.4. In vitro studies

2.4.1. Serum stability

Size exclusion HPLC analysis and an ITLC-SG were used to estimate the serum stability of ^{99m}Tc-N_2S_2-Tat(49–57)-c(RGDyK). A 50 μL volume of labeled peptide solution (0.5 μg /50 μL) was incubated at 37 °C with 1 mL of fresh human serum. Radiochemical stability was determined from 10 μl samples taken at different time points (5 min, 0.5 h and 24 h) for analysis. A shift in the HPLC radioactivity profile to higher molecular weight indicated protein binding, while lower-molecular weight peaks indicated labeled catabolites or serum cysteine binding.

2.4.2. Solid-phase α(v)β(3) binding assay

Microtiter 96-well vinyl assay plates (Corning, NY, USA) were coated with 100 μL/well of a solution of purified human integrin α(v)β(3) (150 ng/mL, Chemicon-Millipore Corporation, Billerica, MA, USA) in coating buffer (25 mM Tris–HCl, pH 7.4, 150 mM NaCl, 1 mM $CaCl_2$, 0.5 mM $MgCl_2$ and 1 mM $MnCl_2$) for 17 h at 4 °C. The plates were washed twice with binding buffer (0.1% bovine serum albumin (BSA) in coating buffer). The wells were blocked for 2 h with 200 μL blocking buffer (1% BSA in coating buffer). The plates were washed twice with binding buffer. Then, 100 μL binding buffer containing 10 kBq of ^{99m}Tc-N_2S_2-Tat(49–57)-c(RGDyK) or ^{99m}Tc-EDDA/HYNIC-E-[c(RGDfK)]$_2$ and appropriate dilutions (from 10000 nM to 0.001 nM of c(RGDfK), Bachem-USA) in binding buffer were incubated in the wells at 37 °C for 1 h. After incubation, the plates were washed three times with binding buffer. The wells were cut out and counted in a gamma counter. IC_{50} values of the RGD peptides were calculated by nonlinear regression analysis. Each data point is the average of five determinations.

2.4.3. Internalization assay and non-specific binding

C6 glioma cancer cells were originally obtained from ATCC (USA). The cells were routinely grown at 37 °C with 5% CO_2 and 100% humidity in RPMI medium supplemented with 10% newborn calf serum and antibiotics (100 μg/mL streptomycin).

C6 cells supplied in fresh medium were diluted to 1×10^6 cells/tube (~0.5 mL) and incubated with approximately 200,000 cpm of ^{99m}Tc-N_2S_2-Tat(49–57)-c(RGDyK) or ^{99m}Tc-EDDA/HYNIC-E-[c(RGDfK)]$_2$ (10 μL, 0.3 nmol total peptide) in triplicate at 37 °C for 2 h. The test tubes were centrifuged (3 min, 500 g) and washed twice with phosphate buffered saline (PBS). Radioactivity in the cell pellet represents both externalized peptide (surface-bound) and internalized peptide (internal membrane-bound radioactivity). The externalized peptide activity was removed with 1 mL of 0.2 M acetic acid/0.5 M NaCl solution added to the resuspended cell pellet. The test tubes were centrifuged, washed with PBS, and re-centrifuged. Pellet activity, as determined in a crystal scintillation well-type detector, was considered as internalization. An aliquot with the initial activity was taken to represent 100%, and the cell uptake activity with respect to this value was then calculated. Non-specific binding was determined in parallel, using 0.05 mM c(RGDfK) (Bachem-USA), which blocked cell receptors.

2.5. In vivo studies

2.5.1. Biodistribution studies

Biodistribution and tumor uptake studies in mice were carried out according to the rules and regulations of the Official Mexican Norm 062-ZOO-1999.

Tumor induction in athymic mice: Athymic male mice (20–22 g) were kept in sterile cages with sterile wood-shaving bedding, constant temperature, humidity, noise and 12:12 light periods. Water and feed (standard PMI 5001 feed) were given ad libitum.

Glioma tumors were induced by subcutaneous injection of C6 cells (1×10^6) resuspended in 0.2 mL of phosphate-buffered saline into the upper back of four 6–7 week-old nude mice. Injection sites were observed at regular intervals for tumor formation and progression.

Biodistribution: ^{99m}Tc-N_2S_2-Tat(49–57)-c(RGDyK) or ^{99m}Tc-EDDA/HYNIC-E-[c(RGDfK)]$_2$ (3.7 MBq in 0.05 mL) was injected into the tail vein of the mice. The mice (n = 3) were sacrificed at 1, 3, 6 and 24 h post-injection. Whole tumor, heart, lung, liver, spleen, kidney, intestine, muscle, bone and blood were rinsed with saline, paper blotted and placed into pre-weighed plastic test tubes. The activity was determined in a well-type scintillation detector (Canberra), along with six 0.5 mL aliquots of the diluted standard representing 100% of the injected activity. Mean activities were used to obtain the percentage of injected dose per gram of tissue (% ID/g). A blocking study was performed in two groups of three athymic nude mice bearing C6 gliomas. One hundred microliters (1 mM) of unlabeled cRGDfK (Bachem) was intraperitoneally administered one hour before intravenous injection of ^{99m}Tc-N_2S_2-Tat(49–57)-c(RGDyK) (n = 3) or ^{99m}Tc-EDDA/HYNIC-E-[c(RGDfK)]$_2$ (n = 3), and complete dissection was carried out 1 h after radiopharmaceutical administration, as described above.

2.5.2. Micro-SPECT/CT imaging studies

Single photon emission computed tomography (SPECT) and X-ray computed tomography (CT) images were acquired at 2 h after ^{99m}Tc-N_2S_2-Tat(49–57)-c(RGDyK) or ^{99m}Tc-EDDA/HYNIC-E-[c(RGDfK)]$_2$ administration in the nude mice with the implanted tumors, using a micro-SPECT/CT scanner (Albira, ONCOVISION, Spain). Mice under 2% isoflurane anesthesia were placed in the prone position, and whole body imaging was performed. The micro-SPECT field of view was 60 mm, a symmetric 20% window was set at 113 keV, and pinhole collimators were used to acquire a planar SPECT image. The image data set was then reconstructed using the ordered subset expectation maximization (OSEM) algorithm with a standard mode parameter as provided by the manufacturer. The CT parameters were 35 kV sure voltage, 700 μA current and 600 micro-CT projections.

2.6. Statistical analysis

Differences between the in vitro cell data for RGD-radiopharmaceuticals were evaluated with Student's t-test.

3. Results

The radiochemical purity of ^{99m}Tc-N_2S_2-Tat(49–57)-c(RGDyK) was 96%±2%, as obtained by ITLC, Sep-Pak and HPLC analysis without post-labeling purification (n>30). The average specific activity was 6.4 GBq/μmol. It is expected that the chelating site yields an $[N_2S_2]^{4-}$ coordination around the $[Tc(O)]^{3+}$ core, forming a negatively charged five-coordinate complex [3]. Protein binding was 1.9%±0.2%, 2.1%±0.2% and 15.7%±1.8% at 5 min, 0.5 h and 24 h, respectively, without ^{99m}Tc transchelation to cysteine, indicating adequate radiopharmaceutical stability towards cysteine present in blood (Fig. 2). However, ^{99m}Tc-N_2S_2-Tat(49–57)-c(RGDyK) binds to plasmatic proteins approximately three times more than ^{99m}Tc-EDDA/HYNIC-E-[c(RGDfK)]$_2$ (0.3%±0.2%, 0.6%±0.3% and 5.6%±0.7% at 5 min, 0.5 h and 24 h, respectively). These data indicate that the positive charges on Tat from the arginines and lysines contained in the amino acid sequence tend to interact faster and more strongly with proteins and that Tat is not targeted to a specific receptor.

The *in vitro* affinity, determined by a competitive binding assay, indicated that the cRGDfK concentration necessary to displace fifty per cent of the ^{99m}Tc-N_2S_2-Tat(49–57)-c(RGDyK) (IC_{50}=4.6±0.2 nM) or ^{99m}Tc-EDDA/HYNIC-E-[c(RGDfK)]$_2$ (IC_{50}=6.7±1.3 nM) from the receptor was the same order of magnitude for both, demonstrating high *in vitro* affinity for the α(v)β(3) integrin in both cases (Fig. 3).

The greater internalization of ^{99m}Tc-N_2S_2-Tat(49–57)-c(RGDyK) (37.5%) compared to that of ^{99m}Tc-EDDA/HYNIC-E-[c(RGDfK)]$_2$ (10%) in the C6 cell line is shown in Table 1, indicating that the hybrid peptide has the ability to penetrate the cell membrane. The specificity of the uptake was confirmed by the receptor blocking study (Table 1). In general, cell internalization was receptor specific with ^{99m}Tc-EDDA/HYNIC-E-[c(RGDfK)]$_2$; in ^{99m}Tc-N_2S_2-Tat(49–57)-c(RGDyK), 18% of the total internalized activity was non-specific, as demonstrated by the blocked cell experiments because of the Tat nuclear localizing sequence (NLS) (Table 1). In this work, the nucleus and the cytoplasm were not separated to quantify nuclear internalization. Nevertheless, it was considered necessary to carry out this test with the purpose of estimating cellular dosimetry because of the ^{99m}Tc-auger electron emission.

Biodistribution studies showed both renal and hepatobiliary excretion of the ^{99m}Tc-N_2S_2-Tat(49–57)-c(RGDyK) and ^{99m}Tc-EDDA/HYNIC-E-[c(RGDfK)]$_2$ complexes. However, the tumor, kidney and liver uptake values were significantly higher for the Tat-radiopharmaceutical with respect to ^{99m}Tc-EDDA/HYNIC-E-[c(RGDfK)]$_2$ (Table 2 and Table 3). Nevertheless, both radiopharmaceuticals showed good specific tumor uptake for C6 cells in athymic mice, which was confirmed with the blocking study. However, ^{99m}Tc-N_2S_2-Tat(49–57)-c(RGDyK) showed a better tumor/blood ratio of 15.5 at 3 h compared to 10.3 for ^{99m}Tc-EDDA/HYNIC-E-[c(RGDfK)]$_2$.

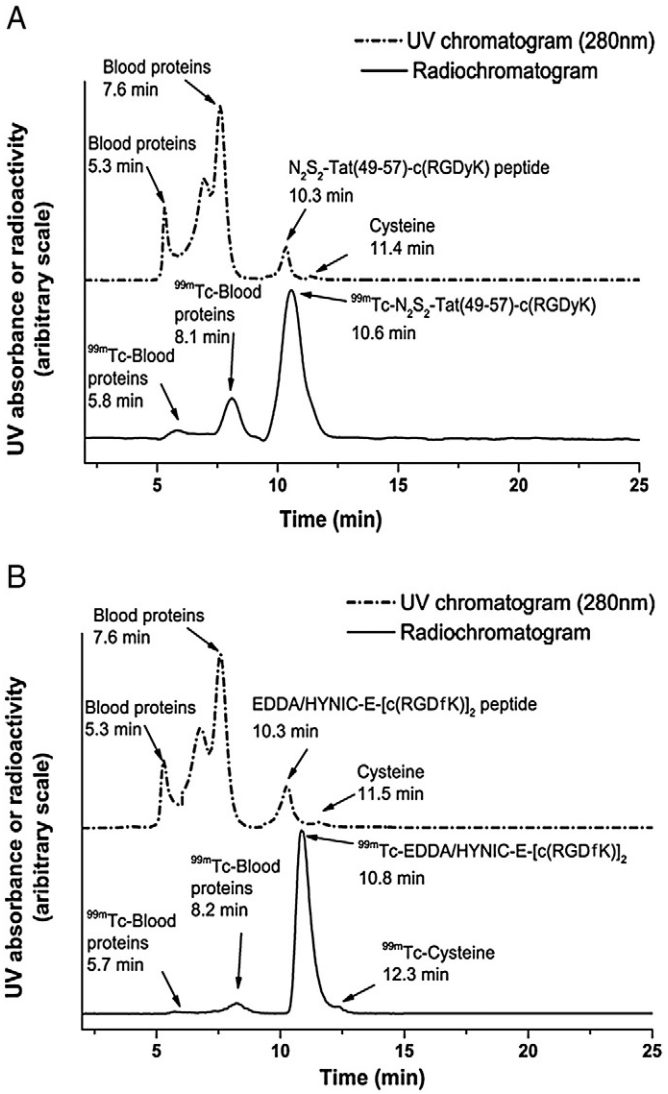

Fig. 2. Size-exclusion HPLC. The solid line represents the UV-chromatogram (280 nm) of human serum proteins and the dotted line represents the radiochromatogram of (A) ^{99m}Tc-N_2S_2-Tat(49–57)-c(RGDyK) or (B) ^{99m}Tc-EDDA/HYNIC-E-[c(RGDfK)]$_2$ at 24 h after incubation in human serum at 37 °C.

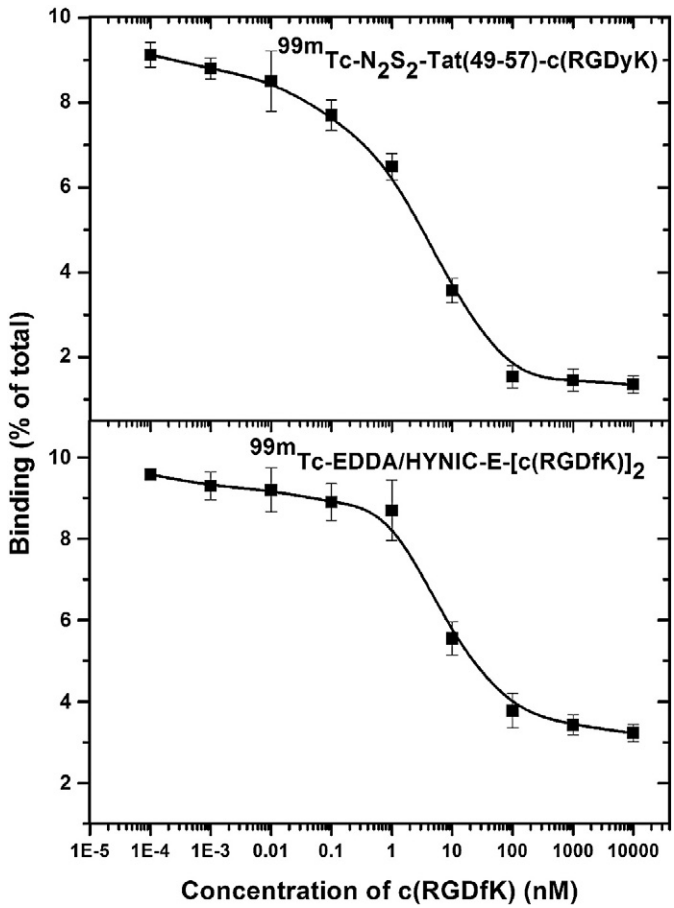

Fig. 3. Competition of ^{99m}Tc-N_2S_2-Tat(49–57)-c(RGDyK) or ^{99m}Tc-EDDA/HYNIC-E-[c(RGDfK)]$_2$ with c(RGDfK) for specific binding to the α(v)β(3) integrin.

Table 1
^{99m}Tc-EDDA/HYNIC-E-[c(RGDfK)]$_2$ and ^{99m}Tc-N_2S_2-Tat(49–57)-c(RGDyK) cell internalization in unblocked and blocked C6 glioma cancer cells at 1 h (% of total activity ± SD, n = 6).

Radiopharmaceutical	Unblocked	Blocked[a]
^{99m}Tc-EDDA/HYNIC-E-[c(RGDfK)]$_2$	10.011 ± 1.726*	2.995 ± 0.332*
^{99m}Tc-N_2S_2-Tat(49–57)-c(RGDyK)	37.499 ± 0.354*	18.541 ± 1.193*

[a] Blocked cells were incubated with an additional integrin receptor blocking dose of c(RGDfK) to determine the non-specific radioactivity binding.
* Significant statistical difference ($p<0.05$) between blocked and unblocked.

A similar behavior was observed with the tumor/muscle ratio of 17 at 3 h for the Tat-radiopharmaceutical compared to 12 for the conventional ^{99m}Tc-RGD peptide (Table 2 and Table 3). An adequate tumor uptake was also observed in the micro-SPECT/CT images obtained at 2 h, in which a good tumor contrast was observed when the ^{99m}Tc-N_2S_2-Tat(49–57)-c(RGDyK) was administered (Fig. 4). The thyroid was found to have a normal biodistribution of RGD peptides.

Table 3
Biodistribution in mice with C6-induced tumors after IV administration of ^{99m}Tc-N_2S_2-Tat(49–57)-c(RGDyK), expressed as a percentage of the injected dose per gram of tissue (% ID/g) (mean ± SD, n = 3).

TISSUE	Unblocked				Blocked[a]
	1 h	3 h	6 h	24 h	1 h
Blood	1.01 ± 0.92	0.45 ± 0.27	0.31 ± 0.10	0.08 ± 0.04	1.15 ± 0.68
Heart	0.93 ± 0.52	0.32 ± 0.12	0.21 ± 0.07	0.09 ± 0.05	0.73 ± 0.65
Lung	1.02 ± 0.41	0.78 ± 0.27	0.29 ± 0.10	0.09 ± 0.03	1.21 ± 0.33
Liver	4.34 ± 0.82	3.86 ± 0.95	3.09 ± 0.58	2.54 ± 0.35	4.81 ± 0.57
Spleen	1.12 ± 0.62	0.98 ± 0.50	0.91 ± 0.36	0.75 ± 0.09	1.08 ± 0.33
Kidney	7.81 ± 0.94	6.51 ± 0.72	6.14 ± 0.68	5.13 ± 0.96	7.94 ± 0.78
Intestine	0.92 ± 0.13	0.78 ± 0.10	0.63 ± 0.09	0.25 ± 0.11	1.08 ± 0.15
Muscle	0.53 ± 0.11	0.41 ± 0.08	0.37 ± 0.07	0.12 ± 0.02	0.46 ± 0.13
Bone	0.61 ± 0.19	0.32 ± 0.10	0.15 ± 0.08	0.06 ± 0.05	0.52 ± 0.14
C6 Tumor	**7.38 ± 1.12***	**6.98 ± 1.34**	**5.48 ± 1.02**	**2.82 ± 0.53**	**3.63 ± 1.26***

[a] Blocked with an additional intraperitoneal cold c(RGDfK) blocking dose 1 h prior to the administration of ^{99m}Tc-N_2S_2-Tat(49–57)-c(RGDyK) to determine the non-specific radioactivity binding.
* Significant difference ($P<0.05$) between unblocked and blocked $\alpha_V\beta_3$ receptors.

4. Discussion

This research demonstrated the high *in vitro* and *in vivo* stability of the ^{99m}Tc-N_2S_2-Tat(49–57)-c(RGDyK) radiopharmaceutical prepared in high radiochemical purity. As previously reported, the $[TcO(N_2S_2)]^{-1}$-Tat(49–57)-peptide structure found at the chelation site has a stable and distorted square pyramidal geometry with the oxo-group at the apical position of the pyramid and Tc in the center of the plane formed by the N_2S_2 donors [3]. This geometry has been found by X-ray diffraction in other five-coordinate Tc(O) complexes, either neutral or charged, such as the negatively charged five-coordinate $Tc(O)N_2S_2$ complexes [14,15].

The HYNIC core with the additional EDDA co-ligand was shown to be highly stable for labeling peptides, as was demonstrated in the case of ^{99m}Tc-EDDA/HYNIC-E-[c(RGDfK)]$_2$ [16–18]. Nevertheless, the technetium-binding region, consisting of the Gly-Gly-Cys-NH_2 peptide (to form an -N_2S_2- ligand), has been successfully used to prepare stable complexes with the $Tc=O^{3+}$ core. Minimum alteration of the molecular bioactivity is in agreement with the results obtained in this research for the ^{99m}Tc-N_2S_2-Tat(49–57)-c(RGDyK) complex [19]. However, the most important advantage of this hybrid radiopharmaceutical is the potential to be used as a diagnostic and therapeutic agent. Low-energy Auger electrons have traditionally been considered to be the most suitable particles for the inactivation of single-spread malignant cells. Previously, we reported that, in the case of ^{99m}Tc, internal conversion (IC) electrons emitting with the highest yield per decay (99.9-88%) and the lowest energy (i.e., 1.82 keV) are the principal contributors to the nuclear-absorbed dose (70.26%). IC electrons could be extremely radiotoxic if they were able to contact DNA, as was expected for the ^{99m}Tc-N_2S_2-Tat(49–57)-c(RGDyK) complex, producing an antiproliferative effect similar to that found for the ^{99m}Tc-N_2S_2-Tat(49–57)-Lys^3-Bombesin [13]. It is also possible that, in the hybrid Tat-RGD radiopharmaceutical, the positive charges on the Tat(49–57) fragment generate an electrostatic interaction with the negatively charged DNA, producing cell toxicity from a biological Auger-effect. Lundqvist et al. [20] have demonstrated that it is important to distinguish between what might be a normal increased cellular dose and the biological Auger effect. Electron energies close to the ionization potential (< 30 eV) will only have a marginal biological effect, and electrons above 5 keV will not contribute to the local effect. For example, an Auger electron with energy of approximately 20 keV is ideal for full deposition within the size of a mammalian cell, but it will be far from DNA and will not have the local DNA impact that is usually associated with the biological Auger-effect, which occurs within cubic nanometers.

The tumors to which ^{99m}Tc-N_2S_2-Tat(49–57)-c(RGDyK) could be successfully applied as a diagnostic and therapeutic agent include: osteosarcoma, neuroblastoma, glioblastoma, melanoma, lung carcinoma and breast cancer, in which the $\alpha(\nu)\beta(3)$ integrin is over-expressed in the tumor cells [7,8]. In the case of breast cancer, the radiopharmaceutical could be administered intratumorally as part of a combined therapy scheme. This scheme could include ^{99m}Tc-N_2S_2-Tat(49–57)-c(RGDyK) and ^{99m}Tc-N_2S_2-Tat(49–57)-Lys^3-Bombesin to simultaneously target two different receptors that are over-expressed in breast cancer, $\alpha(v)\beta(3)$ integrin and the gastrin-releasing peptide receptor. Additionally, cytotoxic analogues of bombesin, in combination with other peptides, could be successfully used to inhibit cancer cell proliferation [21–23].

Table 2
Biodistribution in mice with C6-induced tumors after IV administration of ^{99m}Tc-EDDA/HYNIC-E-[c(RGDfK)]$_2$, expressed as a percentage of the injected dose per gram of tissue (% ID/g) (mean ± SD, n = 3).

TISSUE	Unblocked				Blocked[a]
	1 h	3 h	6 h	24 h	1 h
Blood	0.62 ± 0.44	0.36 ± 0.07	0.23 ± 0.12	0.07 ± 0.01	0.71 ± 0.32
Heart	0.18 ± 0.09	0.11 ± 0.05	0.09 ± 0.02	0.05 ± 0.02	0.23 ± 0.15
Lung	0.31 ± 0.11	0.29 ± 0.07	0.19 ± 0.02	0.18 ± 0.08	0.34 ± 0.11
Liver	2.96 ± 0.78	2.36 ± 0.33	2.27 ± 0.36	2.10 ± 0.19	2.24 ± 0.68
Spleen	0.74 ± 0.28	0.63 ± 0.31	0.70 ± 0.18	0.90 ± 0.10	0.59 ± 0.43
Kidney	4.19 ± 0.94	3.83 ± 0.57	3.98 ± 0.91	2.79 ± 1.03	3.94 ± 1.02
Intestine	1.84 ± 0.72	0.59 ± 0.14	0.48 ± 0.08	0.13 ± 0.09	1.90 ± 0.45
Muscle	0.32 ± 0.07	0.30 ± 0.03	0.23 ± 0.17	0.04 ± 0.02	0.30 ± 0.11
Bone	0.07 ± 0.12	0.11 ± 0.08	0.05 ± 0.07	0.04 ± 0.01	0.11 ± 0.11
C6 Tumor	**4.38 ± 0.88***	**3.72 ± 0.52**	**3.25 ± 0.52**	**1.68 ± 0.44**	**1.63 ± 0.29***

[a] Blocked with an additional intraperitoneal cold c(RGDfK) blocking dose 1 h prior to the administration of ^{99m}Tc-EDDA/HYNIC-E-[c(RGDfK)]$_2$ to determine the non-specific radioactivity binding.
* Significant difference ($P<0.05$) between unblocked and blocked $\alpha_V\beta_3$ receptors.

5. Conclusions

^{99m}Tc-N_2S_2-Tat(49–57)-c(RGDyK) has been developed as a hybrid radiopharmaceutical composed of a penetrating peptide with a specific targeting moiety (Tat conjugated to RGD) producing a stable, labeled molecule able to overcome the lipophilic cell membrane barrier with higher internalization in $\alpha(v)\beta(3)$ integrin-positive cancer cells with respect to ^{99m}Tc-EDDA/HYNIC-E-[c(RGD)]$_2$. Therefore, this hybrid is

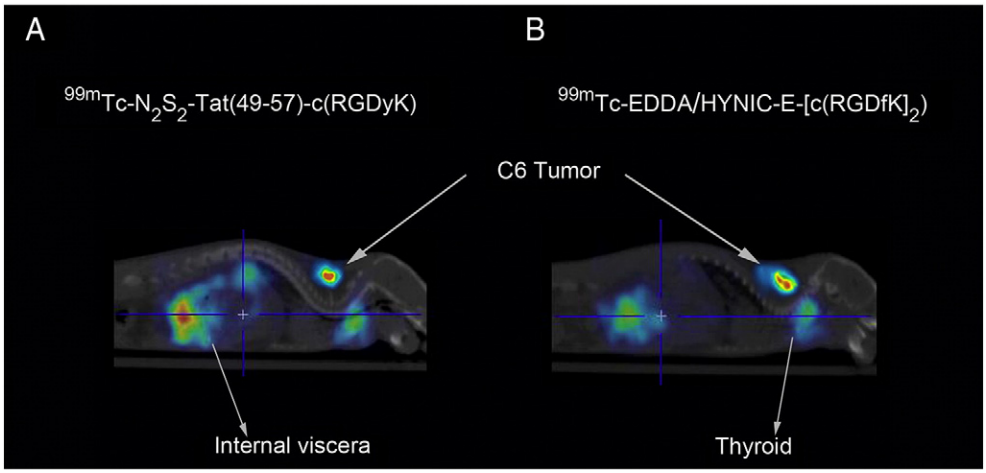

Fig. 4. Micro-SPECT/CT images in athymic mice with C6 induced tumors 2 h after 3.7 MBq intravenous administration of (A) ^{99m}Tc-N_2S_2-Tat(49–57)-c(RGDyK) or (B) ^{99m}Tc-EDDA/HYNIC-E-[c(RGDfK)]$_2$. Mice were anesthetized with 2% isoflurane. Field of view: 60 mm.

potentially useful for imaging and as a possible therapy for tumors expressing α(v)β(3) integrins.

Acknowledgments

This study was supported by the National Council of Science and Technology (CONACYT-SEP-CB-2010-01-150942).

References

[1] Torchilin VP. Tat peptide-mediated intracellular delivery of pharmaceutical nanocarriers. Adv Drug Deliv Rev 2008;60:548–58.
[2] Gump JM, Dowdy SF. TAT transduction: the molecular mechanism and therapeutic prospects. Trends Mol Med 2007;13:443–8.
[3] Santos-Cuevas CL, Ferro-Flores G, Arteaga de Murphy CA, Ramirez de FM, Luna-Gutierrez MA, Pedraza-Lopez M, et al. Design, preparation, *in vitro* and *in vivo* evaluation of ^{99m}Tc-N_2S_2-Tat(49–57)-bombesin: a target-specific hybrid radiopharmaceutical. Int J Pharm 2009;375:75–83.
[4] Mishra A, Lai GH, Schmidt NW, Sun VZ, Rodriguez AR, Tong R, et al. Translocation of HIV TAT peptide and analogues induced by multiplexed membrane and cytoskeletal interactions. Proc Natl Acad Sci USA 2011;108:16883–8.
[5] Buchegger F, Perillo-Adamer F, Dupertuis YM, Bischof A. Auger radiation targeted into DNA: a therapy perspective. Eur J Nucl Med Mol Imaging 2006; 33:1352–63.
[6] Howell R. Radiation spectra for Auger-electron emitting radionuclides: report 2 of AAPM Nuclear Medicine Task Group No. 6. Med Phys 1992;19:1371–83.
[7] Liu S. Radiolabeled multimeric cyclic RGD peptides as integrin alphavbeta3 targeted radiotracers for tumor imaging. Mol Pharm 2006;3:472–87.
[8] Kenny LM, Coombes RC, Oulie I, Contractor KB, Miller M, Spinks TJ, et al. Phase I trial of the positron-emitting Arg-Gly-Asp (RGD) peptide radioligand ^{18}F-AH111585 in breast cancer patients. J Nucl Med 2008;49:879–86.
[9] Haubner R, Decristoforo C. Radiolabeled RGD peptides and peptidomimetics for tumor targeting. Front Biosciences 2009;14:872–86.
[10] Mitrasinovic PM. Advances in α(ν)β(3) integrin-targeting cancer therapy and imaging with radiolabeled RGD peptides. Current Radiopharm 2009;2:214–9.
[11] Morales-Avila E, Ferro-Flores G, Ocampo-Garcia BE, De Leon-Rodriguez LM, Santos-Cuevas CL, Medina L, et al. Multimeric system of ^{99m}Tc-labeled gold nanoparticles conjugated to c[RGDfK(C)] for molecular imaging of tumor α(v)β(3) expression. Bioconjugate Chem 2011;22:913–22.
[12] Luna-Guiterrez M, Ferro-Flores G, Ocampo-Garcia BE, Jimenez-Mancilla NP, Morales-Avila E, De Leon-Rodriguez LM, et al. ^{177}Lu-labeled monomeric, dimeric and multimeric RGD peptides for the therapy of tumors expressing αvβ3 integrins. J Labelled Comp Radiopharm 2012;50:140–8.
[13] Santos-Cuevas CL, Ferro-Flores G, Rojas-Calderon EL, Garcia-Becerra R, Ordaz-Rosado D, Arteaga de Murphy C, et al. ^{99m}Tc-N_2S_2-Tat(49–57)-bombesin internalized in nuclei of prostate and breast cancer cells: kinetics, dosimetry and effect on cellular proliferation. Nucl Med Comm 2011;32:303–13.
[14] Bandoli G, Dolmella A, Porchia M, Refosco F, Tisato F. Structural overview of technetium compounds (1993–1999). Coord Chem Rev 2001;214:43–90.
[15] Canney DJ, Billings J, Francesconi LC, Guo Y-Z, Haggerty BS, Rheingold AL, et al. Dicarboxylate diamide dimercaptide(N_2S_2) technetium-99 m complexes: synthesis and biological evaluation as potential renal radiopharmaceuticals. J Med Chem 1993;36:1032–40.
[16] Decristoforo C, Melendez-Alafort L, Sosabowski JK, Mather SJ. ^{99m}Tc-HYNIC-[Tyr^3]-octreotide for imaging somatostatin-receptor-positive tumors: preclinical evaluation and comparison with ^{111}In-octreotide. J Nucl Med 2000;41:1114–9.
[17] Ferro-Flores G, Murphy CA, Rodriguez-Cortes J, Pedraza-Lopez M, Ramirez-Iglesias MT. Preparation and evaluation of ^{99m}Tc-EDDA/HYNIC-[Lys^3]-bombesin for imaging of GRP receptor-positive tumours. Nucl Med Comm 2006;27:371–6.
[18] Miranda-Olvera AD, Ferro-Flores G, Pedraza-Lopez M, Murphy CA, De Leon-Rodriguez LM. Synthesis of oxytocin HYNIC derivatives as potential diagnostic agents for breast cancer. Bioconjugate Chem 2007;18:1560–7.
[19] Francesconi LC, Zheng Y, Bartis J, Blumenstein M, Costello C, De Rosch MA. Preparation and characterization of [^{99}TcO] apcitide: a technetium labeled peptide. Inorg Chem 2004;43:2867–75.
[20] Lundqvist H, Stenerlöw B, Gedda L. The Auger effect in molecular targeting therapy. In: Stigbrand T, Carlsson J, Adams GP, editors. Targeted radionuclide tumor therapy. NewYork: Springer; 2008. p. 195–214.
[21] Schally AV, Nagy A. Cancer chemotherapy based on targeting of cytotoxic peptide conjugates to their receptors on tumors. Eur J Endocrinol 1999;141:1–14.
[22] Buchholz S, Keller G, Schally AV, Halmos G, Hohla F, Heinrich E, et al. Therapy of ovarian cancers with targeted cytotoxic analogs of bombesin, somatostatin, and luteinizing hormone-releasing hormone and their combinations. Proc Natl Acad Sci USA 2006;103:10403–7.
[23] Ziegler CG, Brown JW, Schally AV, Erler A, Gebauer L, Treszl A, et al. Expression of neuropeptide hormone receptors in human adrenal tumors and cell lines: antiproliferative effects of peptide analogues. Proc Natl Acad Sci USA 2009;106: 15879–84.